Cardiac neurons expressing a glucagon-like receptor mediate cardiac arrhythmia induced by high-fat diet in *Drosophila*

Yunpo Zhao[1,2], Jianli Duan[1,2], Joyce van de Leemput[1,2], Zhe Han[1,2,*]

1. Center for Precision Disease Modeling, Department of Medicine, University of Maryland School of Medicine, Baltimore, MD 21201, USA
2. Division of Endocrinology, Diabetes and Nutrition, Department of Medicine, University of Maryland School of Medicine, Baltimore, MD 21201, USA

* To whom correspondence should be addressed.

Corresponding author:
Dr. Zhe Han, PhD
Center for Precision Disease Modeling
Department of Medicine, University of Maryland School of Medicine
670 West Baltimore Street, Baltimore, MD 21201, USA
Email: zhan@som.umaryland.edu

Short title: Glucagon in HFD-induced cardiac arrhythmia

Keywords: cardiac neurons, AkhR, Adipokinetic hormone (Akh), Glucagon, cardiac arrhythmia, high-fat diet, *Drosophila*

HIGHLIGHTS

- High-fat diet activates Akh (glucagon-like)-producing neurons near the esophagus in *Drosophila*
- Reducing Akh prevents high-fat diet-induced cardiac arrhythmia in flies
- Discovery of two neurons located at the posterior end of the heart that express the Akh receptor (AkhR) and innervate the heart
- Eliminating one of the two AkhR-expressing cardiac neurons (ACN) results in cardiac arrhythmia, whereas the absence of functional AkhR prevents high-fat diet-induced cardiac arrhythmia in flies

ABSTRACT

Cardiac arrhythmia leads to increased risks for stroke, heart failure, and cardiac arrest. Arrhythmic pathology is rooted in the cardiac conduction system, but the mechanism is complex and not fully understood. For example, how metabolic diseases, like obesity and diabetes, increase the risk for cardiac arrhythmia. Glucagon regulates glucose production, mobilizes lipids from the fat body, and affects cardiac rate and rhythm, attributes of a likely key player. *Drosophila* is an established model to study metabolic diseases and cardiac arrhythmias. Since glucagon signaling is highly conserved, we used high-fat diet (HFD)-fed flies to study its effect on heart function. HFD led to increased heartbeat and an irregular rhythm. The HFD-fed flies showed increased levels of adipokinetic hormone (Akh), the functional equivalent to human glucagon. Both genetic reduction of Akh and eliminating the Akh producing cells (APC) rescued HFD-induced arrhythmia, whereas heart rhythm was normal in Akh receptor mutants ($AkhR^{null}$). Furthermore, we discovered a pair of cardiac neurons that express high levels of Akh receptor. These are located near the posterior heart, make synaptic connections at the heart muscle, and regulate heart rhythm. Altogether, this Akh signaling pathway provides new understanding of the regulatory mechanisms between metabolic disease and cardiac arrhythmia.

57 **INTRODUCTION**

58

59 Arrhythmia refers to an irregular, decreased (bradycardia), or increased (tachycardia)
60 heartbeat. Temporary disruption is usually benign, however chronic arrhythmia has been
61 linked to significantly increased risks for stroke, heart failure, and cardiac arrest (Kannel et al.,
62 1998, 1983; Nattel et al., 2014; Roberts-Thomson et al., 2011). Its pathogenesis is rooted in
63 the cardiac conduction system; however, the mechanism is complex and much remains
64 unknown. Two well-established risk factors that directly contribute to the development of
65 cardiovascular disorders and arrhythmia are obesity (Gupta et al., 2022; Powell-Wiley et al.,
66 2021) and diabetes mellites (Aune et al., 2018; Huxley et al., 2011; Lee et al., 2017). In fact,
67 a longitudinal study into obesity (13.7 years mean follow-up; 5,282 participants) found a 4%
68 increased risk for atrial fibrillation (a form of arrhythmia) per 1-unit increased body mass index
69 (Wang et al., 2004). The other major risk factor, diabetes mellitus has been shown to impact
70 the cardiac conduction system, leading to increased risk of developing atrial fibrillation and
71 ventricular arrhythmias (Kannel et al., 1998). A meta-analysis found that patients with diabetes
72 had a 28-40% increased risk for developing atrial fibrillation, with a 20% risk increase reported
73 for pre-diabetic patients (Aune et al., 2018; Huxley et al., 2011). The relationship between
74 higher blood glucose levels and increased risk for atrial fibrillation was dose-responsive (Aune
75 et al., 2018). Diabetes mellites, when considered a cause of disrupted metabolism, as well as
76 obesity have been independently associated with increased risk for atrial fibrillation (Lee et al.,
77 2017). However, to what extent diabetes, blood glucose, and obesity contribute to atrial
78 fibrillation, independently or collectively, and through which pathomechanism requires further
79 study.

80

81 Antagonistic actions by glucagon and insulin regulate glucose metabolism. Besides regulating
82 glucose release from the liver, glucagon facilitates the release of glucose as well as lipids from
83 the fat body, acts as a satiety factor in the central nervous system, affects the glomerular
84 filtration rate, and regulates intra-islet secretion of insulin, glucagon and somatostatin to meet

85 increased energy demands (Habegger et al., 2010; Heppner et al., 2010; Vuguin and Charron,
86 2011). These glucagon regulatory effects are evident in patient studies that showed that an
87 impaired counter-regulatory glucagon response, observed as increased free plasma insulin
88 levels, contributes to glucose instability in patients with long-term diabetes (Scott et al., 1980);
89 that consumption of dietary fats leads to increased plasma glucagon levels in healthy
90 volunteers (Radulescu et al., 2010); and that plasma glucagon levels were significantly higher
91 in people considered obese compared to those considered lean (Stern et al., 2019). Glucagon
92 has been repeatedly shown to affect heart contraction and heart rate. However, the nature of
93 this effect is complex; whether glucagon acts anti- or pro-arrhythmogenic seems to depend on
94 context, such as a non-failing heart or a heart at acute or chronic failure (Neumann et al.,
95 2023). That said, glucagon-producing tumors, *i.e.*, glucagonomas, can cause tachycardia (a
96 form of arrhythmia defined as >100 heart beats per minute) and heart failure without secondary
97 cause (Chang-Chretien et al., 2004; Zhang et al., 2014). Moreover, glucagonoma tumor
98 resection resulted in a normalized heart rate and a return to typical heart size and function
99 (Chang-Chretien et al., 2004). Similarly, glucagon infusion in healthy human volunteers
100 induced arrhythmias (Jaca et al., 2002; Markiewicz et al., 1978). Thus, while glucagon clearly
101 affects heart rhythm, when considering the underlying mechanism much remains unknown.
102
103 The link between high-fat diet (HFD), glucagon, and cardiac arrhythmia is conserved and well-
104 established in animal models. In fact, studies from the 1960s already showed that glucagon
105 increases heart rate in a variety of mammalian species, including dogs, cats, guinea pigs, and
106 rats (Farah and Tuttle, 1960; Lucchesi et al., 1968). More recently, it was shown in mice that
107 both glucagon and the glucagon receptor (Gcgr) are involved in heart rate regulation (Mukharji
108 et al., 2013; Sowden et al., 2007). *Drosophila* adipokinetic hormone (Akh), the functional
109 equivalent to human glucagon, is expressed in a small cluster of endocrine neurons, Akh
110 producing cells (APC) (Kim and Rulifson, 2004; Lee and Park, 2004). These cells in the
111 corpora cardiaca near the esophagus function similar to islet cells in mammals, including the
112 mechanism that regulates hormone secretion, and are essential for larval glucose

homeostasis (Kim and Rulifson, 2004). Like glucagon, Akh is known to also mobilize lipids from the fat body to regulate glucose levels, in the form of trehalose, in the circulating hemolymph to accommodate increased energy demand (Isabel et al., 2005). Likewise, increased Akh increases the heart rate in flies (Noyes et al., 1995). These studies together suggest that glucagon and glucagon signaling, aside from regulating blood sugar levels, play an evolutionarily conserved role in heart rate regulation.

Drosophila melanogaster is a well-established model to study heartbeat and heart arrhythmia (Birse et al., 2010; Ding et al., 2022; Ocorr et al., 2007). For example, HFD-fed flies were used to study the genetic mechanisms of cardiac dysfunction in obesity. It found that HFD leads to reduced cardiac contractility and a reduced heart period (Birse et al., 2010). Notably, this phenotype was attenuated by intervention at the insulin-TOR signaling pathway (Birse et al., 2010), thus supporting a connection between obesity, glucagon, insulin and cardiac function. Here, we used *Drosophila* fed a HFD to study heart arrhythmia. HFD led to increased Akh in the APC of the corpora cardiaca. We then identified a hitherto undescribed pair of cardiac neurons near the posterior heart that highly express the Akh receptor (AkhR) and directly innervate the fly heart. We show that these AkhR cardiac neurons (ACN) regulate heart rhythm in the flies and mediate the HFD-induced arrhythmia. Given the conservation of Akh/glucagon signaling, these findings likely have implications for arrhythmia in patients. Given the significance of the vagus nerve in cardiac rhythm (Ambache and Lippold, 1949; Cai et al., 2023; Freeman, 1951; González et al., 2023; Kharbanda et al., 2023; van Weperen and Vaseghi, 2023) it could fulfill a similar function.

RESULTS

High-fat diet increases heart rate and arrhythmia index

140 All flies (w^{1118}) that eclosed (*i.e.*, adults that emerged from pupa) within 8 hours were sorted
141 (females only) and transferred to fresh food vials (25 flies per vial) containing normal fat diet
142 (NFD) or high-fat diet (HFD, NutriFly diet supplemented with 14% fat) for 7 days. At which
143 point, we determined the heartbeat of the flies using optical coherence tomography (OCT)
144 (Figure 1A). Flies on a HFD show a significantly reduced heart period and increased
145 arrhythmia index compared to NFD-fed flies (Figure 1B-D). These findings are in agreement
146 with previous work (Birse et al., 2010) and indicate that HFD imposes a pathogenic effect on
147 heart function.
148
149 **High-fat diet up-regulates Akh expression and increases Akh producing cell (APC)**
150 **activity**
151 The ingestion of superfluous macronutrients has a great impact on metabolism. We observed
152 enlarged crops, the functional equivalent to the human stomach, in the HFD-fed flies (Figure
153 2-figure supplement 1). We asked whether the metabolic signaling pathways contributed to
154 the HFD-caused pathogenic effect on the heart. Akh, the functional equivalent to human
155 glucagon, is expressed by a group of neuroendocrine cells known as APC in the corpora
156 cardiaca (Lee and Park, 2004). Indeed, flies that carried *Akh*-Gal4 to express GFP showed
157 Akh producing cells at the corpora cardiaca, which attaches to the esophagus, just anterior to
158 the proventriculus (Figure 2A). Quantitative PCR showed that the expression of *Akh* was
159 significantly up-regulated in the flies fed a HFD, compared to NFD-fed flies (Figure 2B).
160
161 Next, to test whether the HFD-induced increase in Akh in the APC affects APC neuron activity,
162 we used CaLexA (Masuyama et al., 2012). A basal level of CaLexA fluorescence was
163 observed in the APC of NFD-fed flies, while a significantly higher fluorescence was detected
164 in the APC of HFD-fed flies (Figure 2C, D). This shows that HFD increases APC neuron
165 activity. Taken together, our data show that HFD activates Akh expression in the APC and
166 increases APC activity.
167

168 **Akh regulates heartbeat**

169 To confirm the importance of APC activity and Akh release by the APC, we down-regulated
170 *Akh* (*Akh*-Gal4>UAS-*Akh*-RNAi) and analyzed its effect on heart function. As expected, upon
171 *Akh* depletion in the APCs, the difference in arrhythmia between the NFD and HFD-fed flies
172 disappeared (Figure 3A, B). The findings indicate that the endocrine signal Akh, originating in
173 the APC neurons, mediates the HFD cardiac functional pathogenicity.

174

175 **AkhR mediates the high-fat diet pathogenic effect on the heartbeat**

176 Akh binds its receptor AkhR, a G-protein coupled receptor, to activate the signaling pathway
177 (Staubli et al., 2002). We quantified *AkhR* expression using RT-qPCR and observed
178 significantly up-regulated expression in HFD-fed flies (Figure 4A). To confirm its role in Akh-
179 mediated HFD-induced arrhythmia, we tested *AkhR* null mutant flies ($AkhR^{null}$). In line with Akh
180 depletion, flies with *AkhR* mutation and fed a HFD, did not show the HFD-associated cardiac
181 arrhythmia (Figure 4B, C). These data show that Akh/AkhR signaling mediates the pathogenic
182 effect of HFD on heart function.

183

184 **A pair of AkhR cardiac neurons (ACN) are associated with the heart**

185 To determine the AkhR expression pattern, we used *AkhR*-Gal4 (Lee et al., 2018) to drive the
186 expression of GFP. The adipose fat body tissue is a major organ that expresses AkhR at the
187 embryonic and larval stages (Grönke et al., 2007), as well as in the adult (Bharucha et al.,
188 2008). Likewise, we observed GFP fluorescence in the fat body in *AkhR*-Gal4>*GFP* flies
189 (Figure 5A, B). Notably, no fluorescence was detected in the cardiac muscles. However, we
190 did find two neurons with strong GFP fluorescence, indicative of high expression levels of
191 AkhR, located near the posterior end of the heart tube (Figure 5B). These neurons had
192 elaborate neurites along the heart tube (Figure 5B-D) and formed synaptic connections with
193 heart muscles, as revealed by immunostaining for active zone marker Bruchpilot (Brp) (Figure
194 5E, F). These two neurons likely communicate with the heart muscle via these neuromuscular
195 junctions. Therefore, were refer to these two neurons as AkhR cardiac neurons (ACN).

196

197 **Partial elimination of AkhR cardiac neurons (ACN) causes arrhythmia**

198 To determine the function of the ACN, we set out to eliminate the pair. We overexpressed
199 UAS-*rpr* under control of *AkhR*-Gal4 to induce apoptosis. We observed one remaining AkhR
200 cardiac neuron in the *AkhR*-Gal4>UAS-*rpr* flies (Figure 6A), indicating partial elimination. The
201 *AkhR*-Gal4>UAS-*rpr* flies were subjected to OCT analysis. The profile and rhythm of the
202 heartbeat were drastically affected in the flies with only one ACN (Figure 6B). This
203 demonstrates the importance of the ACN in regulating the heartbeat.

204

205

206 **DISCUSSION**

207

208 **The role of AkhR, glucagon-like receptor, in regulating heart rate and rhythm**

209 Heart function is dependent on glucose as an energy source. Glucagon converts stored
210 glycogen, in the liver and fat tissue, into glucose that is released into the blood stream/ Its link
211 to cardiac arrhythmia has been well-established. The glucose signaling pathway is conserved
212 across species, including *Drosophila* (Kim and Rulifson, 2004). Like in humans, in flies the
213 glucagon-like hormone Akh regulates the glucose levels in hemolymph (fly equivalent to blood)
214 (Kim and Rulifson, 2004). Under starvation conditions, Akh mobilizes glycogen and lipids to
215 maintain the circulatory glucose levels. The flies become hyperactive and show increased food
216 searching behavior. Flies without Akh, either by depletion or APC elimination, show starvation
217 resistant behavior, suggesting that the behavioral change is mediated by Akh (Huang et al.,
218 2020; Lee and Park, 2004; Yu et al., 2016). Notably, in flies fed a HFD, the AkhR expressing
219 neurons in the brain become hypersensitive to Akh stimulation, due to upregulated AkhR
220 (Huang et al., 2020). Finally, prepupae injected with low pharmacological doses of Akh, *i.e.*,
221 doses higher than physiologically expected, showed increased heart rates (Noyes et al.,
222 1995). Thus, in both humans and flies, heart rate and rhythm respond to nutritional changes

223 (flies, see Figure 1), this mechanism likely supports the higher metabolic demands and
224 possibly mediates the switch from glucose to stored lipids as the main energy source.
225
226 To date, studies have focused on the direct effect of glucagon on cardiac tissue, based on the
227 notion that cardiomyocytes express glucagon receptors (GCGR). However, evidence of
228 GCGR expression in human heart tissue has been conflicting. No cardiac signal was detected
229 when using radioactively labeled glucagon (Bomholt et al., 2022), results of mRNA data have
230 been inconsistent (Aranda-Domene et al., 2023; Bomholt et al., 2022), and protein data for
231 GCGR to support cardiac expression is lacking (Neumann et al., 2023). Here, we identified an
232 endocrine neuron-heart axis using a fly model for high-fat diet-induced arrhythmia. In this fly
233 model (Figure 7), the consumption of a HFD elevates the expression of Akh, a glucagon-like
234 hormone, and activity of the APC. The elevated circulatory Akh is transported to the AkhR
235 cardiac neurons (ACN) located near the posterior end of the heart, where the increased
236 signaling leads to an escalated heart arrhythmia index. These findings revealed a hitherto
237 undescribed regulatory signaling pathway that links the consumption of superfluous
238 macronutrients with heart arrhythmia.
239
240 **Cardiac regulatory neurons in *Drosophila***
241 *Drosophila* have a cardiac cycle that consists of alternating retrograde and anterograde heart
242 beats that correlate to the multi-chamber diastole and systole, respectively (Dulcis and Levine,
243 2005). Accordingly, two signaling systems that innervate the fly heart were identified. The
244 retrograde beat being regulated by glutamatergic innervation. Its transverse nerves run
245 bilaterally along the longitudinal muscle and innervate the cardiac muscles of the conical
246 chamber as well as the alary muscles (Dulcis and Levine, 2005, 2003). The anterograde
247 heartbeat being regulated by crustacean cardioactive peptide (CCAP) innervation. Its bipolar
248 neurons (BpN) extent CCAP fibers that innervate each segment of the abdominal heart. Four
249 additional large CCAP-positive neurons innervate the terminal chamber (Dulcis et al., 2005;
250 Dulcis and Levine, 2003). These earlier studies, leave the possibility of synaptic input or

251 hormonal regulation of the BpN neurosecretory signals to the heart. The authors comment on
252 the absence of direct descending input from the corpora cardiaca to the *Drosophila* abdominal
253 heart as has been observed in other systems (Dulcis and Levine, 2003). Here, we identified
254 corpora cardiaca released Akh signaling to previously unreported AkhR cardiac neurons
255 (ACN) that could exercise this function in flies. Given their localization at the terminal end of
256 the cardiac chamber, where the four large CCAP-positive neurons are located as well, it is
257 possible that the ACN modulate CCAP signaling at the heart. In fact, the previous study
258 detected synaptotagmin on the BpN (BpN6) cell bodies which suggests the presence of
259 presynaptic sites (Dulcis and Levine, 2003). We are currently investigating if the BpN and ACN
260 act together, whether in concert or opposingly.
261
262 **Relevance of findings in fly for humans**
263 This study revealed how glucagon-like hormone Akh is released by APCs in response to HFD
264 and stimulates AkhR cardiac neurons (ACN) to regulate heart rhythm in flies. Like in the flies,
265 glucagon infusion in healthy human volunteers induces arrhythmias (Jaca et al., 2002;
266 Markiewicz et al., 1978). Moreover, a preliminary study in infants and children demonstrated
267 the potential of glucagon to treat atrioventricular (AV) block, a heart rhythm disorder marked
268 by a slow heart rate caused by dysfunctional electrical conduction (Hurwitz, 1973). Clinical
269 guidelines by the American Heart Association recommend the use of glucagon to treat
270 bradycardia due to beta-blocker or calcium channel blocker overdose (Kusumoto et al., 2019).
271 However, the mechanism by which glucagon exerts these beneficial clinical effects remains
272 poorly understood. Our findings implicate a potentially conserved signaling pathway in which
273 elevated glucagon leads to increased cardiac neuronal activity and subsequent increased
274 heart rate and arrhythmia. Multiple trials are investigating the possible benefits of glucagon
275 receptors (GCGR) agonists alone or in combination with GLP-1 agonists to treat arrhythmia,
276 but so far the results have been mixed. An initial trial with a GCGR antagonist in patients with
277 type 2 diabetes was halted prematurely due to the detrimental side effects, which included
278 elevated blood cholesterol and steatosis (liver dysfunction) (Agrawal and Gupta, 2016; Kazda

279 et al., 2016a, 2016b; Pearson et al., 2016). Our findings provide new possible glucagon-
280 related targets for treating obesity-associated cardiac arrhythmia by targeting cardiac neurons
281 receptive to glucagon signaling rather than the cardiomyocytes as had been the leading
282 hypothesis to date. Studies into the human equivalent of ACN would be interesting; possibly
283 the vagus nerve could fulfill a similar function as its importance for cardiac rhythm has been
284 firmly established (Ambache and Lippold, 1949; Cai et al., 2023; Freeman, 1951; González et
285 al., 2023; Kharbanda et al., 2023; van Weperen and Vaseghi, 2023).
286
287 Finally, while the exact implications of these findings for new therapeutics remain to be seen,
288 they do support the avoidance of a high-fat diet. If unavoidable, for example in the case of a
289 therapeutic ketogenic diet or in the subset of patients with diabetes that have elevated
290 glucagon blood levels (D'Alessio, 2011; Unger et al., 1970), then targeting the glucagon
291 pathway might protect against harmful cardiac side effects.
292
293
294 **MATERIALS AND METHODS**
295
296 **Key resources table**

Reagent type (species) or resource	Designation	Source or reference	Identifiers	Additional information
Antibody	anti-Brp (mouse IgG1, kappa light chain)	Developmental Studies Hybridoma Bank	Cat# Nc82 RRID: AB_2314866	IF (1:100)
Antibody	goat anti-mouse Alexa Fluor 647	Jackson Immunoresearch Laboratories	Cat# 102643-594	IF (1:500)
Other	Alexa Fluor 647 Phalloidin	ThermoFisher	Cat# A22287	IF (1:1000)
Other	normal goat serum	Jackson Immunoresearch Laboratories	Cat# 102643-594	1% in 1xPBST
Genetic reagent (*Drosophila melanogaster*)	w^{1118}	Bloomington Drosophila Stock Center	BDSC_3605	
Genetic reagent (*Drosophila melanogaster*)	*Akh*-Gal4	Bloomington Drosophila Stock Center	BDSC_25684	

Genetic reagent (*Drosophila melanogaster*)	UAS-*Akh*-RNAi	Bloomington Drosophila Stock Center	BDSC_34960	
Genetic reagent (*Drosophila melanogaster*)	w^{1118} P{UAS-rpr.C}27; P{UAS-2x*EGFP*}AH3	Bloomington Drosophila Stock Center	BDSC_ 91417	
Genetic reagent (*Drosophila melanogaster*)	*AkhR*^{null}	Bloomington Drosophila Stock Center	BDSC_80937	
Genetic reagent (*Drosophila melanogaster*)	w[*]; P{w[+mC]=LexAop-CD8-GFP-2A-CD8-GFP}2; P{w[+mC]=UAS-*mLexA-VP16-NFAT*}H2, P{w[+mC]=lexAop-rCD2-GFP}3/TM6B, Tb[1]	Bloomington Drosophila Stock Center	BDSC_66542	
Genetic reagent (*Drosophila melanogaster*)	*10x*UAS-*GFP*	Bloomington Drosophila Stock Center	BDSC_32185	
Genetic reagent (*Drosophila melanogaster*)	*AkhR-T2A*-Gal4	Bloomington Drosophila Stock Center	BDSC_78877	
Chemical compound, drug	4% paraformaldehyde (PFA)	Thermo Fisher Scientific	Cat# J19943.K2	
Chemical compound, drug	Triton X-100	Sigma-Aldrich	Cat# 9002-93-1	0.2% in 1xPBS
Chemical compound, drug	4′,6-Diamidino-2-phenylindole (DAPI)	Thermo Fisher Scientific	Cat# D1306 RRID: AB_2629482	(0.5 µg/ml)
Commercial assay or kit	10x phosphate buffered saline	Quality Biological	Cat# 119-069-131	
Commercial assay or kit	TRIzol	Thermo Fisher Scientific	Cat# 15596026	
Commercial assay or kit	EcoDry Premix kit	Takara Bio	Cat# 639549	
Commercial assay or kit	PowerSYBR Green	Applied Biosystems - Thermo Fisher Scientific	Cat# 4367659	
Commercial assay or kit	VECTASHIELD	Vector Laboratories	Cat# H-1000	
Software, algorithm	Adobe Illustrator 2022	Adobe Inc.	RRID:SCR_010279	
Software, algorithm	ImageJ	National Institutes of Health	RRID:SCR_003070	
Software, algorithm	GraphPad Prism9	GraphPad	RRID:SCR_002798	

297

298

299 ***Drosophila* husbandry**

300 *Drosophila* were reared on a normal fat diet (NFD, Nutri-Fly German formula; Genesee
301 Scientific, San Diego, CA; 66-115) or a high-fat diet (HFD, NFD supplemented with 14%
302 coconut oil), under standard conditions (25°C, 60% humid, 12h:12h dark:light). The following
303 fly lines were obtained from Bloomington Drosophila Stock Center (BDSC) at Indiana
304 University Bloomington (Bloomington, IN): w^{1118} (BDSC_3605), *Akh*-Gal4 (BDSC_25684),
305 UAS-*Akh*-RNAi (BDSC_34960), *Akh-T2A*-Gal4 (BDSC_78877), w^{1118} P{UAS-*rpr.C*}27;
306 P{UAS-2x*EGFP*}AH3 (BDSC_91417), $AkhR^{null}$ (BDSC_80937), *w[*]; P{w[+mC]=LexAop-*
307 *CD8-GFP-2A-CD8-GFP}2; P{w[+mC]*=UAS-*mLexA-VP16-NFAT}H2, P{w[+mC]=lexAop-*
308 *rCD2-GFP}3/TM6B, Tb[1]* (BDSC_66542), and *10x*UAS-*GFP* (BDSC_32185).

309

310 **Optical coherence tomography (OCT)**

311 Cardiac function in adult *Drosophila* was measured using an OCT system (Bioptigen; this
312 system was built by the Biophotonics Group, Duke University, Durham, NC (Yelbuz et al.,
313 2002)). For this, newly eclosed adult flies (female) were transferred to fresh vials containing
314 NFD or HFD for 7 days. The flies were anesthetized by carbon dioxide (CO_2) and mounted
315 onto a glass slide using fixogum rubber cement (Marabu GmbH & Co. KG, Tamm, Germany;
316 MR290117000). The flies were allowed to recover for 10 minutes and then imaged using OCT.
317 The flies were scanned at the cardiac chamber in abdominal segment A2. The acquisition
318 parameters were as follows: 48 Hz, 800 frames.

319

320 **Quantification of heart period and arrhythmia index**

321 The heart period and arrhythmia index were quantified as previously reported (Ocorr et al.,
322 2007) with minor modifications. In brief, the OCT raw data was processed using ImageJ
323 software (version 2.9.0/1.53) (Schneider et al., 2012). Within each OCT image (10 seconds)
324 the heart periods were arranged by length. The heart period value for each fly was based on
325 the average of three short, three medium and three long heart periods (*i.e.*, nine periods in

326 total). The arrhythmia index for a genotype was based on the group average (7-day-old
327 females; n=11-23), presented with the standard deviation (SD).
328
329 **Immunostaining and confocal imaging**
330 Flies were dissected in 1xPBS, then fixed in 4% PFA for 30 at room temperature. The
331 specimens were then washed in PBST (0.2% Triton X-100 in 1xPBS) three times, 15 min
332 each, followed by blocking in 1% normal goat serum (Jackson ImmunoResearch Laboratories,
333 West Grove, PA; 102643-594) in PBST for 1 hour at room temperature. The specimens were
334 incubated in primary antibody at 4°C overnight, then washed in PBST three times 15 min.
335 Next, the specimens were incubated in secondary antibody for 2 hours at room temperature,
336 followed by three 15 min washes in PBST, followed by a 10 min wash in PBS. DAPI staining
337 (Thermo Fisher Scientific, Waltham, MA; D1306, 0.5 µg/ml in PBST) was performed in-
338 between the washing steps after the secondary antibody staining. The following antibodies
339 were used: mouse monoclonal anti-Brp 1:100 (Developmental Studies Hybridoma Bank, Iowa
340 City, IA; nc82, RRID:AB_2314866); goat anti-mouse Alexa Fluor 647 1:500 (Jackson
341 ImmunoResearch Laboratories, West Grove, PA; 115-605-003). Alexa Fluor 647 Phalloidin
342 1:1,000 (Thermo Fisher Scientific, Waltham, MA; A22287) was used to stain the filament actin.
343 Antibodies were diluted in the blocking buffer. The specimens were mounted with Vectashield
344 antifade mounting media (Vector Laboratories, Newark, CA; H-1000). The samples were
345 imaged using a ZEISS LSM 900 confocal microscope and ZEISS ZEN blue edition (version
346 3.0) acquisition software under a 20x Plan-Apochromat 0.8 N.A. air objective or a 63x Plan-
347 Apochromat 1.4 N.A. oil objective. For quantitative comparison of intensities, settings were
348 chosen to avoid oversaturation (using range indicator in ZEN blue) and applied across images
349 for all samples within an assay. Image J was used for image processing (version 2.9.0/1.53t;
350 National Institutes of Health, Bethesda, MD) (Schneider et al., 2012).
351
352 **Reverse Transcriptase-quantitative PCR (RT-qPCR)**

353 For quantification of Akh and AkhR mRNA levels, adult female flies fed NFD or HFD for 7 days
354 were transferred into 1.5 mL Eppendorf tubes (10 flies/tube) and flash frozen in liquid nitrogen.
355 Total RNA was extracted using TRIzol (Thermo Fisher Scientific, Waltham, MA, Cat#
356 15596026) according to the manufacturer's protocol. In brief, 0.5 mL TRIzol was added to
357 each tube, then flies were grinded using a pestle. Following, 0.1 ml chloroform was added,
358 sample tubes securely capped, and vigorously shaken by hand for 15 seconds. Samples were
359 incubated at 22°C for 2 minutes, then centrifuged at 12,000x*g* for 15 minutes at 4°C, and
360 supernatants transferred to a clean tube in which total RNA was precipitated using isopropanol
361 (Sigma-Aldrich, St. Louis, MO; 67-63-0). Synthesis of cDNA using reverse transcriptase was
362 performed with the RNA to cDNA EcoDry Premix kit (Takara Bio, San Jose, CA; 639549) and
363 and the subsequent quantitative PCR using PowerSYBR Green (Applied Biosystems - Thermo
364 Fisher Scientific, Waltham, MA; 4367659), according to the manufacturers' protocols. qPCR
365 was performed using a QuantStudio 6 Pro Real-Time PCR machine (Thermo Fisher Scientific,
366 Waltham, MA). The following primers (5'-3') were used: Akh_F
367 TTTCGAGACACAGCAGGGCA, with Akh_R GGTGCTTGCAGTCCAGAAA; AkhR_F
368 ACAATCCGTCGGTGAACA, with AkhR_R CATCACCTGGCCTCTTCCAT. For each
369 treatment, three biological replicates were prepared. ΔΔCT method was used to quantify the
370 gene expression levels with normalization to *Ribosomal protein L32* (*RpL32*) as internal
371 reference gene (Rpl32_F AACCGCGTTTACTGCGGCGA, with Rpl32_R
372 AGAACGCAGGCGACCGTTGG).
373
374 **CaLexA assays**
375 CaLexA assays were performed to determine the neuron activity. *Akh*-Gal4 virgins were
376 crossed with CaLexA males (*w[*]; P{w[+mC]=LexAop-CD8-GFP-2A-CD8-GFP}2;*
377 *P{w[+mC]*=UAS-*mLexA-VP16-NFAT}H2, P{w[+mC]=lexAop-rCD2-GFP}3/TM6B, Tb[1]*) and
378 maintained on NFD. The newly eclosed adults were transferred to fresh food vials containing
379 NFD or HFD for 3 days. The flies were then dissected in 1x phosphate buffered saline (1xPBS)
380 (Quality Biological, Gaithersburg, MD; 119-069-131) at room temperature and fixed in 4%

381 paraformaldehyde (PFA) (Thermo Fisher Scientific, Waltham, MA; J19943.K2) in 1xPBS for 1
382 hour at room temperature, followed by three 15 min washes in 1xPBS with Triton X-100
383 (Sigma-Aldrich, St. Louis, MO; 9002-93-1) (PBST). The specimens were then stained in DAPI
384 (0.5 µg/ml in PBST) (Thermo Fisher Scientific, Waltham, MA; D1306) for 10 min and washed
385 once for 15 min in 1xPBS before mounting with Vectashield antifade mounting media (Vector
386 Laboratories, Newark, CA; H-1000). The samples were imaged using a ZEISS LSM 900
387 confocal microscope and ZEISS ZEN blue edition (version 3.0) acquisition software under a
388 20x Plan-Apochromat 0.8 N.A. air objective a 63x Plan-Apochromat 1.4 N.A. oil objective. For
389 quantitative comparison of intensities, settings were chosen to avoid oversaturation (using
390 range indicator in ZEN blue) and applied across images for all samples within an assay. Image
391 J was used for image processing (version 2.9.0/1.53t; National Institutes of Health, Bethesda,
392 MD) (Schneider et al., 2012).
393
394 **Data analysis and figure preparation**
395 Figures were arranged using Adobe Illustrator software (version 26.2.1; Adobe Inc., San Jose,
396 CA). The relative fluorescence intensity was acquired using ImageJ software (version
397 2.9.0/1.53t; National Institutes of Health, Bethesda, MD) (Schneider et al., 2012). Data plotting
398 and statistical analyses were performed using Prism 9 (GraphPad Software, Boston, MA).
399 Data normality was tested by using the Shapiro-Wilk test. Normally distributed data were
400 analyzed by Student's *t*-test with Welch's correction (two groups) or by a one-way ANOVA
401 followed by Dunnett's correction or two-way ANOVA corrected with Sidak. P-value < 0.05 was
402 considered significant.
403
404
405
406
407
408

ACKNOWLEDGMENTS

We would like to thank the Bloomington Drosophila Stock Center (BDSC) based at Indiana University Bloomington (Bloomington, IN) for the *Drosophila* stocks and the Developmental Studies Hybridoma Bank (DSHB) based at the University of Iowa (Iowa City, IA) for providing the antibodies.

FUNDING

This work was supported by National Institutes of Health grants NHLBI R01-HL134940 (ZH) and NICHD R01-HD111480 (ZH).

DATA AVAILABILITY

All relevant data can be found within the article and its supplementary information.

AUTHOR CONTRIBUTIONS

YZ and HZ designed the project; YZ and JD carried out the experiments; YZ carried out the data analyses; YZ prepared the figures; YZ and JvdL wrote the draft and revisions; HZ provided project oversight, resources, and funding. The manuscript has been critically reviewed and the final version approved by all authors.

ORCIDs: Yunpo Zhao (0000-0002-7942-3406); Jianli Duan (0000-0001-7347-4774); Joyce van de Leemput (0000-0003-1903-7295); Zhe Han (0000-0002-5177-7798)

DISCLOSURES

The authors declare no competing interests.

REFERENCES

Agrawal S, Gupta Y. 2016. Comment on Kazda et al. Evaluation of Efficacy and Safety of the Glucagon Receptor Antagonist LY2409021 in Patients With Type 2 Diabetes: 12- and 24-Week Phase 2 Studies. Diabetes Care 2016;39:1241-1249. *Diabetes Care*.

Ambache N, Lippold OC. 1949. Bradycardia of central origin produced by injections of tetanus toxin into the vagus nerve. *J Physiol* **108**:186–196.

Aranda-Domene R, Orenes-Piñero E, Arribas-Leal JM, Canovas-Lopez S, Hernández-Cascales J. 2023. Evidence for a lack of inotropic and chronotropic effects of glucagon and glucagon receptors in the human heart. *Cardiovasc Diabetol* **22**:128.

Aune D, Feng T, Schlesinger S, Janszky I, Norat T, Riboli E. 2018. Diabetes mellitus, blood glucose and the risk of atrial fibrillation: A systematic review and meta-analysis of cohort studies. *J Diabetes Complications* **32**:501–511.

Bharucha KN, Tarr P, Zipursky SL. 2008. A glucagon-like endocrine pathway in Drosophila modulates both lipid and carbohydrate homeostasis. *J Exp Biol* **211**:3103–3110.

Birse RT, Choi J, Reardon K, Rodriguez J, Graham S, Diop S, Ocorr K, Bodmer R, Oldham S. 2010. High-fat-diet-induced obesity and heart dysfunction are regulated by the TOR pathway in Drosophila. *Cell Metab* **12**:533–544.

Bomholt AB, Johansen CD, Christensen JB, Kjeldsen SAS, Galsgaard KD, Winther-Sørensen M, Serizawa R, Hornum M, Porrini E, Pedersen J, Ørskov C, Gluud LL, Sørensen CM, Holst JJ, Albrechtsen R, Wewer Albrechtsen NJ. 2022. Evaluation of commercially

465 available glucagon receptor antibodies and glucagon receptor expression. *Commun*
466 *Biol* **5**:1278.
467 Cai C, Wu N, Yang G, Yang S, Liu W, Chen M, Po SS, TREAT PVC investigators. 2023.
468 Transcutaneous electrical vagus nerve stimulation to suppress premature ventricular
469 complexes (TREAT PVC): study protocol for a multi-center, double-blind, randomized
470 controlled trial. *Trials* **24**:683.
471 Chang-Chretien K, Chew JT, Judge DP. 2004. Reversible dilated cardiomyopathy associated
472 with glucagonoma. *Heart* **90**:e44.
473 D'Alessio D. 2011. The role of dysregulated glucagon secretion in type 2 diabetes. *Diabetes*
474 *Obes Metab* **13 Suppl 1**:126–132.
475 Ding M, Li QF, Yin G, Liu JL, Jan XY, Huang T, Li AC, Zheng L. 2022. Effects of Drosophila
476 melanogaster regular exercise and apolipoprotein B knockdown on abnormal heart
477 rhythm induced by a high-fat diet. *PLoS One* **17**:e0262471.
478 Dulcis D, Levine RB. 2005. Glutamatergic Innervation of the Heart Initiates Retrograde
479 Contractions in Adult Drosophila melanogaster. *J Neurosci* **25**:271–280.
480 Dulcis D, Levine RB. 2003. Innervation of the heart of the adult fruit fly, Drosophila
481 melanogaster. *J Comp Neurol* **465**:560–578.
482 Dulcis D, Levine RB, Ewer J. 2005. Role of the neuropeptide CCAP in Drosophila cardiac
483 function. *J Neurobiol* **64**:259–274.
484 Farah A, Tuttle R. 1960. Studies on the pharmacology of glucagon. *J Pharmacol Exp Ther*
485 **129**:49–55.
486 Freeman AG. 1951. Electrocardiographic findings during operative manipulation of the viscera
487 and vagus nerves. *Lancet* **1**:926–930.
488 González ML, Pividori SM, Fosser G, Pontecorvo AA, Franco-Riveros VB, Tubbs RS,
489 Boezaart AP, Reina MA, Buchholz B. 2023. Innervation of the heart: Anatomical study
490 with application to better understanding pathologies of the cardiac autonomics. *Clin*
491 *Anat* **36**:550–562.
492 Grönke S, Müller G, Hirsch J, Fellert S, Andreou A, Haase T, Jäckle H, Kühnlein RP. 2007.

493 Dual lipolytic control of body fat storage and mobilization in Drosophila. *PLoS Biol*
494 **5**:e137.
495 Gupta V, Munjal JS, Jhajj P, Jhajj S, Jain R. 2022. Obesity and Atrial Fibrillation: A Narrative
496 Review. *Cureus* **14**:e31205.
497 Habegger KM, Heppner KM, Geary N, Bartness TJ, DiMarchi R, Tschöp MH. 2010. The
498 metabolic actions of glucagon revisited. *Nat Rev Endocrinol* **6**:689–697.
499 Heppner KM, Habegger KM, Day J, Pfluger PT, Perez-Tilve D, Ward B, Gelfanov V, Woods
500 SC, DiMarchi R, Tschöp M. 2010. Glucagon regulation of energy metabolism. *Physiol*
501 *Behav* **100**:545–548.
502 Huang R, Song T, Su H, Lai Z, Qin W, Tian Y, Dong X, Wang L. 2020. High-fat diet enhances
503 starvation-induced hyperactivity via sensitizing hunger-sensing neurons in Drosophila.
504 *Elife* **9**:e53103.
505 Hurwitz RA. 1973. Effect of glucagon on infants and children with atrioventricular heart block.
506 *Br Heart J* **35**:1260–1264.
507 Huxley RR, Filion KB, Konety S, Alonso A. 2011. Meta-analysis of cohort and case-control
508 studies of type 2 diabetes mellitus and risk of atrial fibrillation. *Am J Cardiol* **108**:56–
509 62.
510 Isabel G, Martin JR, Chidami S, Veenstra JA, Rosay P. 2005. AKH-producing neuroendocrine
511 cell ablation decreases trehalose and induces behavioral changes in Drosophila. *Am*
512 *J Physiol Regul Integr Comp Physiol* **288**:R531-8.
513 Jaca IJ, Desai D, Barkin JS. 2002. Paroxysmal supraventricular tachycardia after
514 administration of glucagon during upper endoscopy. *Gastrointest Endosc* **56**:304.
515 Kannel WB, Abbott RD, Savage DD, McNamara PM. 1983. Coronary heart disease and atrial
516 fibrillation: the Framingham Study. *Am Heart J* **106**:389–396.
517 Kannel WB, Wolf PA, Benjamin EJ, Levy D. 1998. Prevalence, incidence, prognosis, and
518 predisposing conditions for atrial fibrillation: population-based estimates. *Am J Cardiol*
519 **82**:2N-9N.
520 Kazda CM, Ding Y, Kelly RP, Garhyan P, Shi C, Lim CN, Fu H, Watson DE, Lewin AJ,

521 Landschulz WH, Deeg MA, Moller DE, Hardy TA. 2016a. Evaluation of Efficacy and
522 Safety of the Glucagon Receptor Antagonist LY2409021 in Patients With Type 2
523 Diabetes: 12- and 24-Week Phase 2 Studies. *Diabetes Care* **39**:1241–1249.
524 Kazda CM, Ding Y, Kelly RP, Garhyan P, Shi C, Lim CN, Fu H, Watson DE, Lewin AJ,
525 Landschulz WH, Deeg MA, Moller DE, Hardy TA. 2016b. Response to Comment on
526 Kazda et al. Evaluation of Efficacy and Safety of the Glucagon Receptor Antagonist
527 LY2409021 in Patients With Type 2 Diabetes: 12- and 24-Week Phase 2 Studies.
528 Diabetes Care 2016;39:1241-1249. *Diabetes Care*.
529 Kharbanda RK, Ramdat Misier NL, van Schie MS, Zwijnenburg RD, Amesz JH, Knops P,
530 Bogers AJJC, Taverne YJHJ, de Groot NMS. 2023. Insights Into the Effects of Low-
531 Level Vagus Nerve Stimulation on Atrial Electrophysiology: Towards Patient-Tailored
532 Cardiac Neuromodulation. *JACC Clin Electrophysiol* **9**:1843–1853.
533 Kim SK, Rulifson EJ. 2004. Conserved mechanisms of glucose sensing and regulation by
534 Drosophila corpora cardiaca cells. *Nature* **431**:316–320.
535 Kusumoto FM, Schoenfeld MH, Barrett C, Edgerton JR, Ellenbogen KA, Gold MR,
536 Goldschlager NF, Hamilton RM, Joglar JA, Kim RJ, Lee R, Marine JE, McLeod CJ,
537 Oken KR, Patton KK, Pellegrini CN, Selzman KA, Thompson A, Varosy PD. 2019.
538 2018 ACC/AHA/HRS Guideline on the Evaluation and Management of Patients With
539 Bradycardia and Cardiac Conduction Delay: Executive Summary: A Report of the
540 American College of Cardiology/American Heart Association Task Force on Clinical
541 Practice Guidelines, and the Heart Rhythm Society. *Circulation* **140**:e333–e381.
542 Lee G, Park JH. 2004. Hemolymph sugar homeostasis and starvation-induced hyperactivity
543 affected by genetic manipulations of the adipokinetic hormone-encoding gene in
544 Drosophila melanogaster. *Genetics* **167**:311–323.
545 Lee H, Choi E-K, Lee S-H, Han K-D, Rhee T-M, Park C-S, Lee S-R, Choe W-S, Lim W-H,
546 Kang S-H, Cha M-J, Oh S. 2017. Atrial fibrillation risk in metabolically healthy obesity:
547 A nationwide population-based study. *Int J Cardiol* **240**:221–227.
548 Lee P-T, Zirin J, Kanca O, Lin W-W, Schulze KL, Li-Kroeger D, Tao R, Devereaux C, Hu Y,

549 Chung V, Fang Y, He Y, Pan H, Ge M, Zuo Z, Housden BE, Mohr SE, Yamamoto S,
550 Levis RW, Spradling AC, Perrimon N, Bellen HJ. 2018. A gene-specific T2A-GAL4
551 library for Drosophila. *Elife* **7**. doi:10.7554/eLife.35574
552 Lucchesi BR, Brown J, Laidlaw B, Rockiki D. 1968. Cardiac Actions of Glucagon. *Circ Res*
553 **22**:777–787.
554 Markiewicz K, Cholewa M, Górski L. 1978. Cardiac arrhythmias after intravenous
555 administration of glucagon. *Eur J Cardiol* **6**:449–458.
556 Masuyama K, Zhang Y, Rao Y, Wang JW. 2012. Mapping neural circuits with activity-
557 dependent nuclear import of a transcription factor. *J Neurogenet* **26**:89–102.
558 Mukharji A, Drucker DJ, Charron MJ, Swoap SJ. 2013. Oxyntomodulin increases intrinsic
559 heart rate through the glucagon receptor. *Physiol Rep* **1**:e00112.
560 Nattel S, Guasch E, Savelieva I, Cosio FG, Valverde I, Halperin JL, Conroy JM, Al-Khatib SM,
561 Hess PL, Kirchhof P, De Bono J, Lip GYH, Banerjee A, Ruskin J, Blendea D, Camm
562 AJ. 2014. Early management of atrial fibrillation to prevent cardiovascular
563 complications. *Eur Heart J* **35**:1448–1456.
564 Neumann J, Hofmann B, Dhein S, Gergs U. 2023. Glucagon and Its Receptors in the
565 Mammalian Heart. *Int J Mol Sci* **24**. doi:10.3390/ijms241612829
566 Noyes BE, Katz FN, Schaffer MH. 1995. Identification and expression of the Drosophila
567 adipokinetic hormone gene. *Mol Cell Endocrinol* **109**:133–141.
568 Ocorr K, Reeves NL, Wessells RJ, Fink M, Chen H-SV, Akasaka T, Yasuda S, Metzger JM,
569 Giles W, Posakony JW, Bodmer R. 2007. KCNQ potassium channel mutations cause
570 cardiac arrhythmias in Drosophila that mimic the effects of aging. *Proc Natl Acad Sci*
571 *U S A* **104**:3943–3948.
572 Pearson MJ, Unger RH, Holland WL. 2016. Clinical Trials, Triumphs, and Tribulations of
573 Glucagon Receptor Antagonists. *Diabetes Care*.
574 Powell-Wiley TM, Poirier P, Burke LE, Després J-P, Gordon-Larsen P, Lavie CJ, Lear SA,
575 Ndumele CE, Neeland IJ, Sanders P, St-Onge M-P, Null N. 2021. Obesity and
576 Cardiovascular Disease: A Scientific Statement From the American Heart Association.

577 *Circulation* **143**:e984–e1010.
578 Radulescu A, Gannon MC, Nuttall FQ. 2010. The effect on glucagon, glucagon-like peptide-
579 1, total and acyl-ghrelin of dietary fats ingested with and without potato. *J Clin*
580 *Endocrinol Metab* **95**:3385–3391.
581 Roberts-Thomson KC, Lau DH, Sanders P. 2011. The diagnosis and management of
582 ventricular arrhythmias. *Nat Rev Cardiol* **8**:311–321.
583 Schneider CA, Rasband WS, Eliceiri KW. 2012. NIH Image to ImageJ: 25 years of image
584 analysis. *Nat Methods* **9**:671–675.
585 Scott RS, Espiner EA, Donald RA, Ellis MJ. 1980. Free insulin, C-peptide and glucagon
586 profiles in insulin dependent diabetes mellitus. *Aust N Z J Med* **10**:146–150.
587 Sowden GL, Drucker DJ, Weinshenker D, Swoap SJ. 2007. Oxyntomodulin increases intrinsic
588 heart rate in mice independent of the glucagon-like peptide-1 receptor. *Am J Physiol*
589 *Regul Integr Comp Physiol* **292**:R962-70.
590 Staubli F, Jorgensen TJD, Cazzamali G, Williamson M, Lenz C, Sondergaard L, Roepstorff P,
591 Grimmelikhuijzen CJP. 2002. Molecular identification of the insect adipokinetic
592 hormone receptors. *Proc Natl Acad Sci U S A* **99**:3446–3451.
593 Stern JH, Smith GI, Chen S, Unger RH, Klein S, Scherer PE. 2019. Obesity dysregulates
594 fasting-induced changes in glucagon secretion. *J Endocrinol* **243**:149–160.
595 Unger RH, Aguilar-Parada E, Müller WA, Eisentraut AM. 1970. Studies of pancreatic alpha
596 cell function in normal and diabetic subjects. *J Clin Invest* **49**:837–848.
597 van Weperen VYH, Vaseghi M. 2023. Cardiac vagal afferent neurotransmission in health and
598 disease: review and knowledge gaps. *Front Neurosci* **17**:1192188.
599 Vuguin PM, Charron MJ. 2011. Novel insight into glucagon receptor action: lessons from
600 knockout and transgenic mouse models. *Diabetes Obes Metab* **13 Suppl 1**:144–150.
601 Wang TJ, Parise H, Levy D, D'Agostino RB, Wolf PA, Vasan RS, Benjamin EJ. 2004. Obesity
602 and the Risk of New-Onset Atrial Fibrillation. *JAMA* **292**:2471–2477.
603 Yelbuz TM, Choma MA, Thrane L, Kirby ML, Izatt JA. 2002. Optical coherence tomography:
604 a new high-resolution imaging technology to study cardiac development in chick

605 embryos. *Circulation* **106**:2771–2774.
606 Yu Y, Huang R, Ye J, Zhang V, Wu C, Cheng G, Jia J, Wang L. 2016. Regulation of starvation-
607 induced hyperactivity by insulin and glucagon signaling in adult Drosophila. *Elife*
608 **5**:e15693.
609 Zhang K, Lehner LJ, Praeger D, Baumann G, Knebel F, Quinkler M, Roepke TK. 2014.
610 Glucagonoma-induced acute heart failure. *Endocrinol Diabetes Metab Case Rep*
611 **2014**:140061.
612
613
614
615
616
617
618
619
620
621
622
623
624
625
626
627
628
629
630
631
632

633 **FIGURES**

634

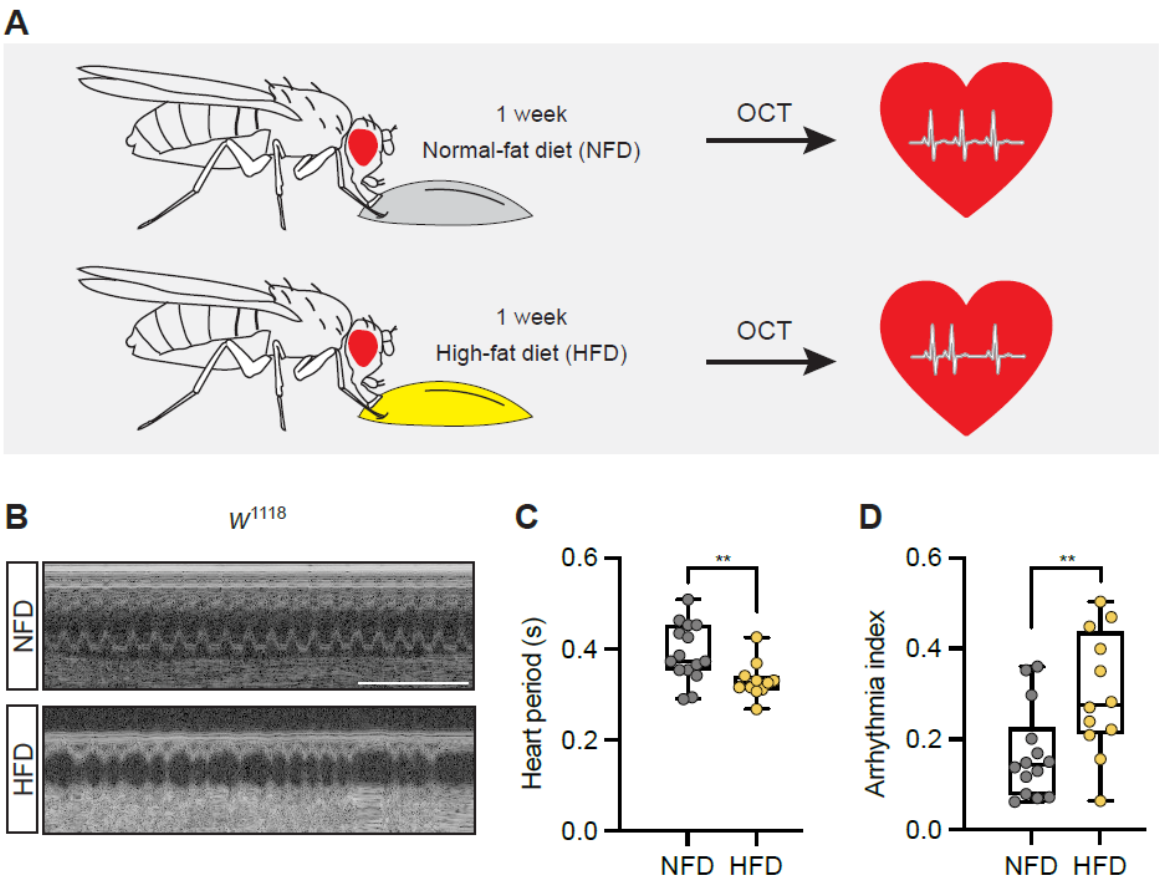

635

636

637 **Figure 1. HFD increases heart rate and arrhythmia index in *Drosophila***

638 **(A)** Schematic illustration of the experimental design. Adult flies (female) were fed either a
639 normal fat diet (NFD) or a high-fat diet (HFD) for 7 days following eclosion from pupa, then
640 subjected to heart functional analysis using optical coherence tomography (OCT) to determine
641 the heart period and the arrhythmia index. **(B)** Representative images obtained from OCT
642 videos of w^{1118} flies that were fed NFD or HFD as indicated. Scale bars: 2 seconds. **(C,D)**
643 Quantitation of heart period (**C**; n=15 NFD, n=11 HFD) and arrhythmia index (**D**; n=14 NFD,
644 n=12 HFD). Statistical analysis was performed using *t*-test corrected with Welch; **, P<0.01.

645

646

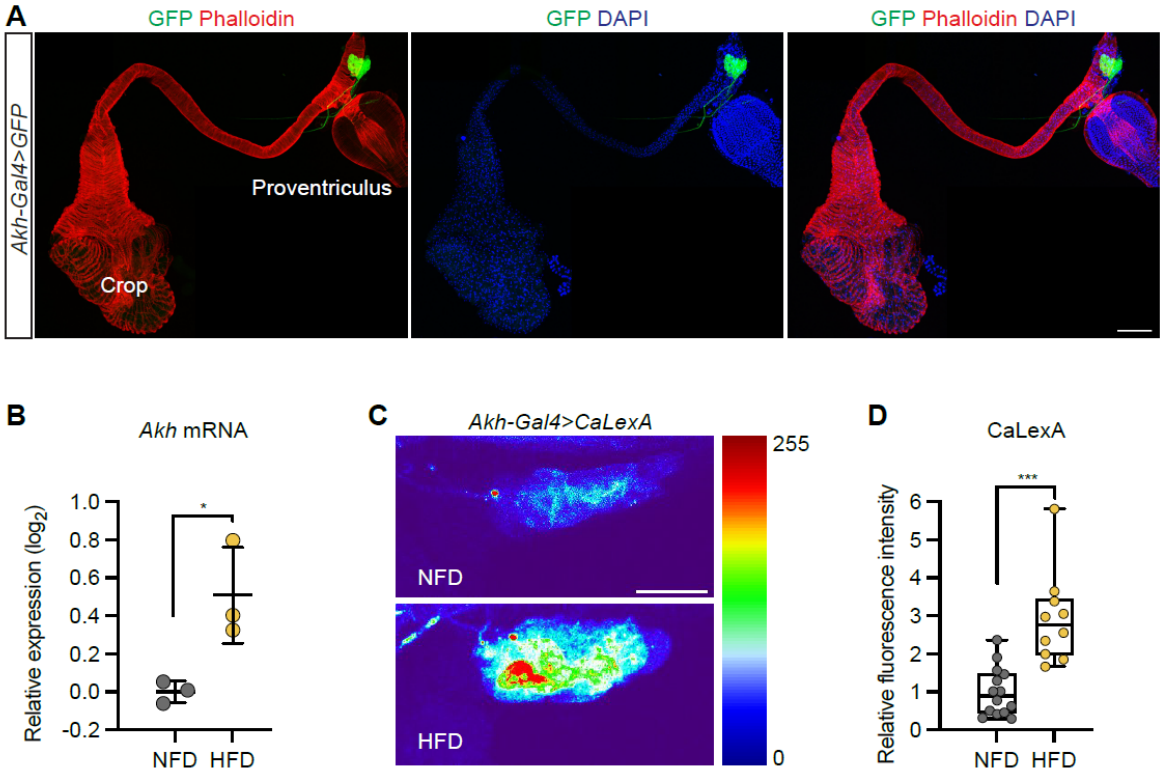

Figure 2. HFD up-regulates adipokinetic hormone gene *Akh* and activates Akh neurons **(A)** Representative confocal image of Akh producing cells (APCs; green, GFP) in *Akh*-Gal4>10xUAS-*GFP* (*Akh*-Gal4>*GFP*) transgenic flies (3-day-old females). The image shows the anterior section of the digestive system, including the crop, esophagus, and proventriculus. The APCs are located at the corpora cardiaca, which attaches to the esophagus, just anterior to the proventriculus. Phalloidin stains actin filaments red; DAPI stains DNA in nucleus blue. Scale bar: 100 μm. **(B)** RT-qPCR analysis of *Akh* expression in w^{1118} flies (female) that were fed either a normal fat diet (NFD) or a high-fat diet (HFD) for 7 days following eclosion from pupa. Ten flies per group, repeated three times. Statistical analysis was performed with unpaired *t*-test corrected with Welch; *, P<0.05. **(C)** Representative confocal images of *Akh*-Gal4>*CaLexA* APCs from female adult flies fed an NFD or HFD (for 7 days following eclosion from pupa). CaLexA is a transcription-based genetically encoded calcium indicator for neuronal activity. CaLexA fluorescence has been presented as heatmap; scale from 0 (blue), no CaLexA detected, to 255 (red) high levels CaLexA. Scale bars: 20 μm. **(D)** Quantitation of CaLexA fluorescence in C (7-day-old females; NFD, n=14; HFD, n=10). Statistical analysis was performed with unpaired *t*-test corrected with Welch; ***, P<0.001.

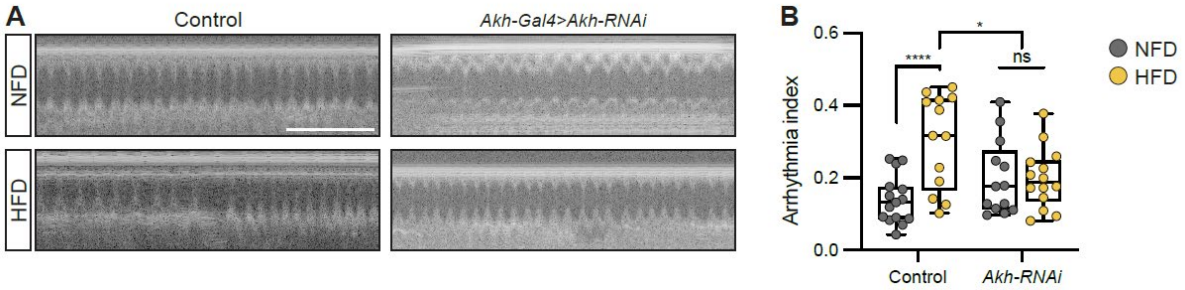

Figure 3. Akh regulates the heartbeat

(A) Representative images obtained from optical coherence tomography (OCT) videos of control (*Akh*-Gal4) and *Akh*-RNAi (*Akh*-Gal4>UAS-*Akh*-RNAi) flies (females, 7 days old) that were fed a normal fat diet (NFD) or a high-fat diet (HFD), as indicated, for seven days starting at eclosion from pupa. Scale bars: 2 seconds. **(B)** Quantitation of the arrhythmia index in control (n=15 NFD, n=13 HFD) and *Akh*-RNAi (n=13 NFD, n=14 HFD) flies. Statistical analysis was performed with two-way ANOVA corrected with Sidak. Statistical significance: *, $p<0.05$; ****, $p<0.0001$; ns, not significant.

688

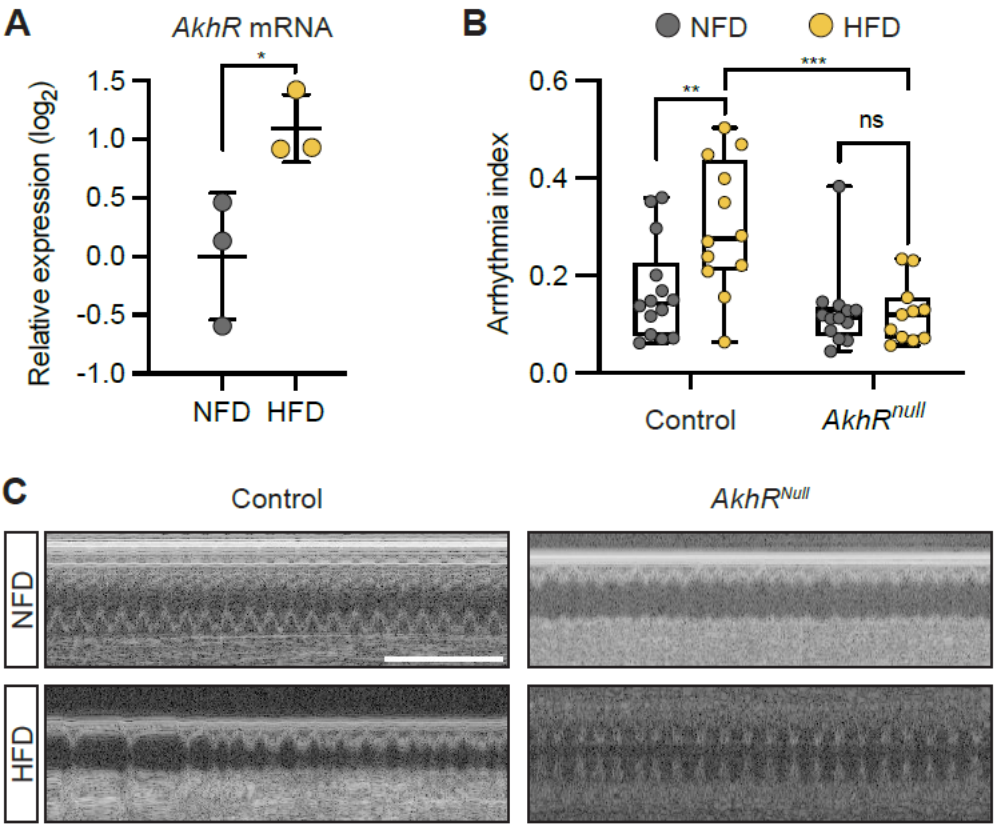

689

690

691 **Figure 4. AkhR regulates the heartbeat**

692 **(A)** RT-qPCR analysis of *AkhR* expression in w^{1118} flies (female) that were fed either a normal
693 fat diet (NFD) or a high-fat diet (HFD) for 7 days following eclosion from pupa. Ten flies per
694 group, repeated three times. Statistical analysis was performed with unpaired *t*-test corrected
695 with Welch; *, P<0.05. **(B)** Quantitation of arrhythmia index in control (n=14 NFD, n=12 HFD)
696 and $AkhR^{null}$ (n=11 NFD, n=13 HFD) flies. Statistical analyses were performed with two-way
697 ANOVA corrected with Sidak; **, P<0.01; ***, P<0.001; ns, not significant. **(C)** Representative
698 images obtained from optical coherence tomography (OCT) videos of control (w^{1118}) and
699 $AkhR^{null}$ mutant flies flies (females, 7 days old) that were fed NFD or HFD, as indicated, for
700 seven days starting at eclosion from pupa. Scale bars: 2 seconds.

701

702

703

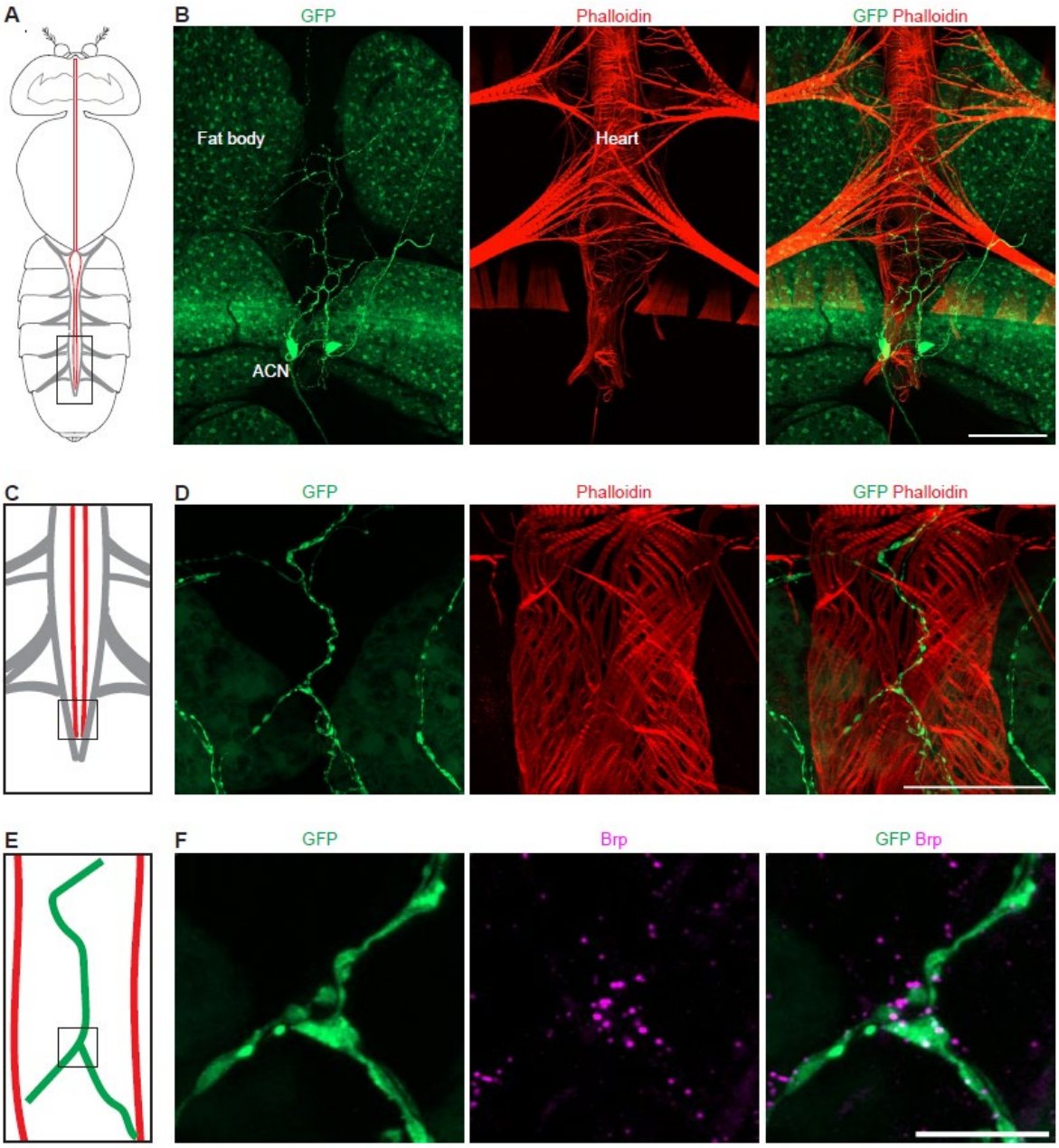

704

705

706 **Figure 5. AkhR cardiac neurons (ACNs) form synaptic connections with the posterior**

707 **heart**

708 **(A)** Graphic depiction of the body (no legs or wings) of an adult fly with the head oriented

709 towards the top. The heart tube (red) is located along the midline in the abdomen (bottom of

710 graphic), with the alary muscles that connect the heart to the exoskeleton represented in light

711 grey. **(B)** A representative confocal image of an *AkhR*-Gal4>10xUAS-*GFP* adult fly (7-day-old,

712 female). The dorsal region of an abdomen corresponding to the boxed region in (A) is shown.

713 *AkhR*>*GFP* labels AkhR in green. ACN, AkhR cardiac neuron. Phalloidin stains actin filaments

714 red. Scale bar: 100 μm. **(C)** Schematic illustration of the posterior fly heart. Corresponds to
715 boxed region in (A). **(D)** A representative confocal image of the posterior heart of an *AkhR*-
716 Gal4>10xUAS-*GFP* fly (7-day-old, female) corresponding to the boxed region in (C).
717 *AkhR*>*GFP* labels AkhR in green. Phalloidin stains actin filaments red. Scale bar: 50 μm. **(E)**
718 Schematic illustration of the posterior end of an adult fly heart. The neurites of the cardiac
719 neurons are depicted in green. Relates to the boxed region in (C). **(F)** Confocal image of the
720 posterior heart of an *AkhR*-Gal4>10xUAS-*GFP* fly (7-day-old, female) corresponding to the
721 boxed region in (E). *AkhR*>*GFP* labels AkhR in green. Anti-Bruchpilot (Brp), a marker for the
722 active zone, is shown in magenta. Scale bar: 10 μm.
723
724
725
726
727
728
729
730
731
732
733
734
735
736
737
738
739
740
741

742

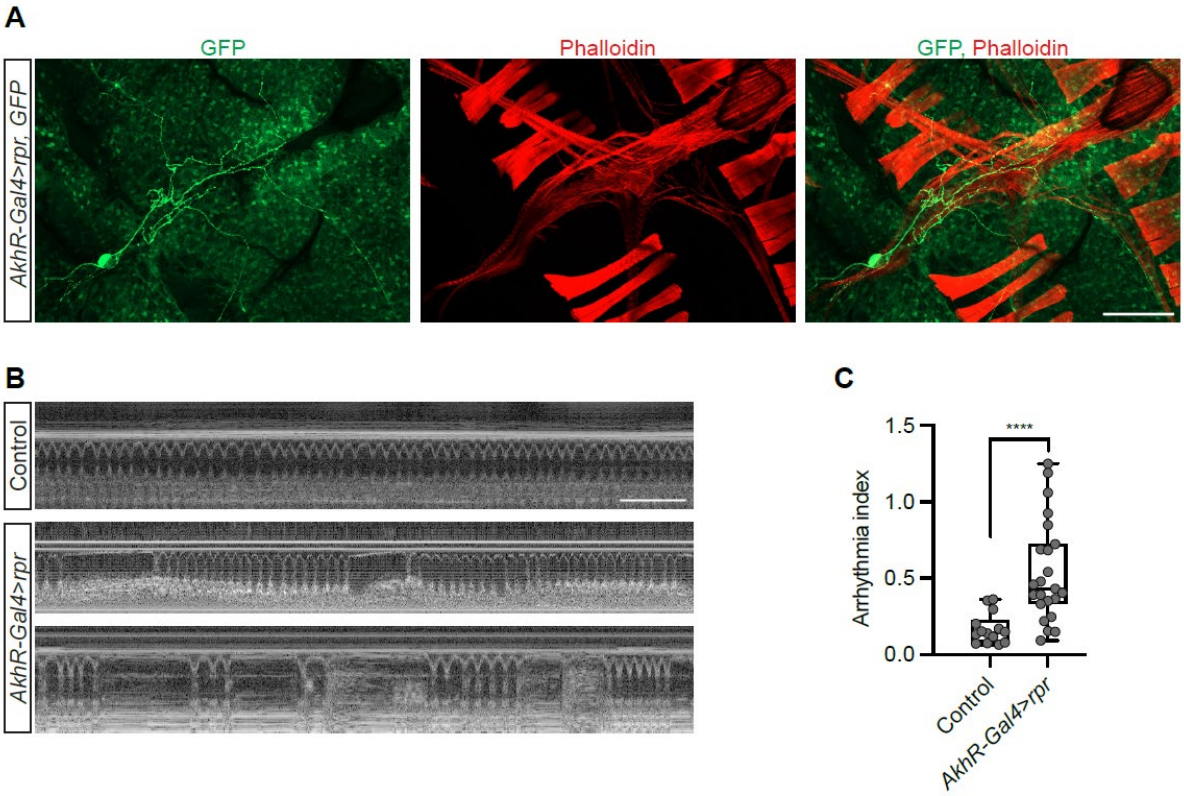

743

744 **Figure 6. Partial elimination of ACNs causes arrhythmia**

745 **(A)** A representative confocal image of an adult *AkhR*-Gal4>*rpr*, *GFP* (*AkhR*-Gal4>UAS-*rpr,*
746 UAS-*GFP*) fly (7-day-old, female). *AkhR*>*GFP* labels AkhR in green. *AkhR*, *adipokinetic*
747 *hormone receptor*; *rpr*, *reaper*. Phalloidin stains actin filaments red. Scale bar: 100 μm. **(B)**
748 Representative images obtained from optical coherence tomography (OCT) videos of control
749 (w^{1118}) and *AkhR*-Gal4>*rpr* (*AkhR*-Gal4>UAS-*rpr,* UAS-*GFP*) flies (7-day-old, female). Scale
750 bar: 2 seconds. **(B)** Quantitation of arrhythmia index in control (n=14 NFD) and *AkhR*-Gal4>*rpr*
751 (n=23 NFD). Statistical analysis was performed using *t*-test corrected with Welch; ****,
752 P<0.0001.

753

754

755

756

757

758

759

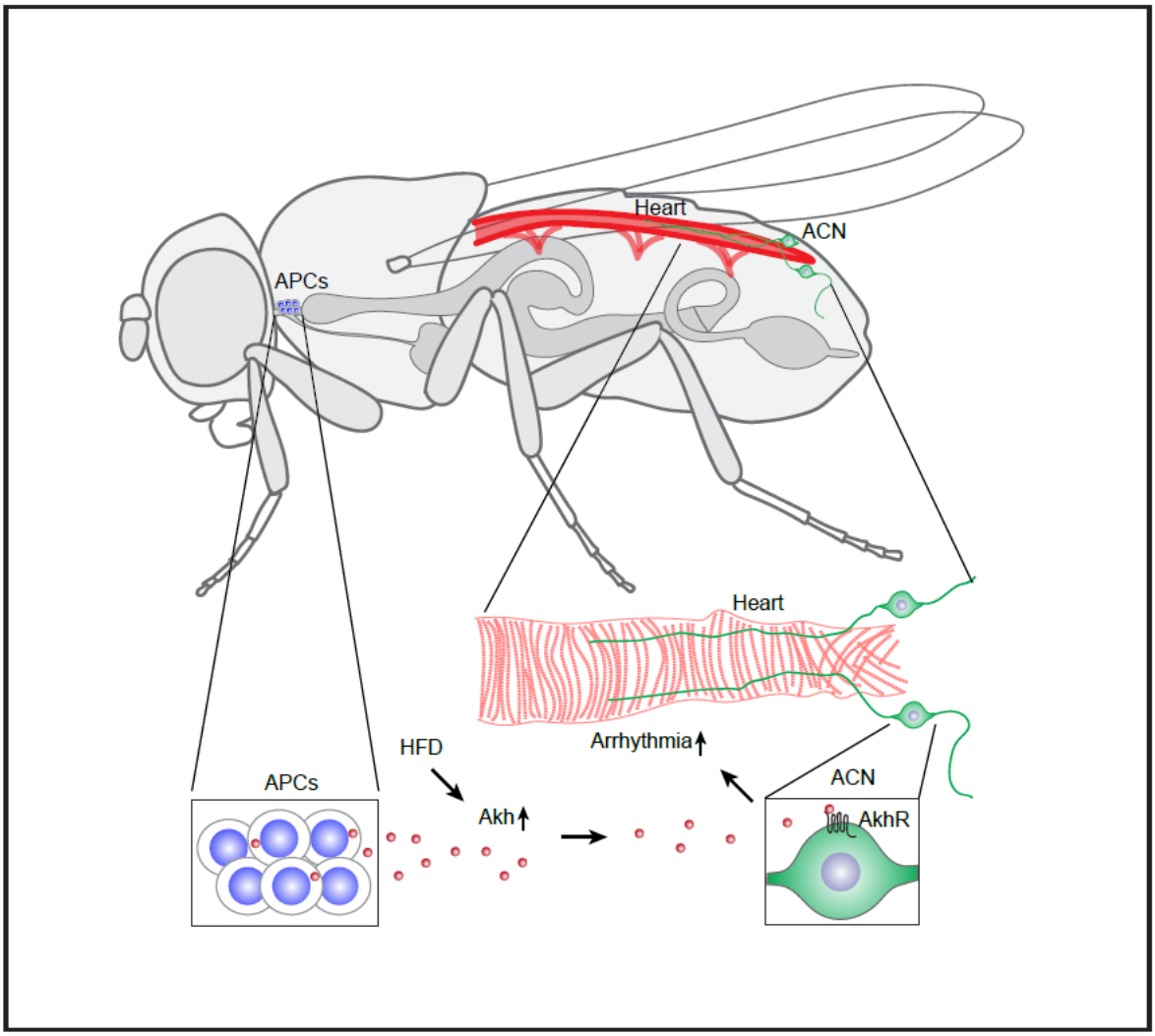

760

761

762 **Figure 7. Model: Akh/AkhR mediates the HFD-induced cardiac arrhythmia**

763 A high-fat diet (HFD) upregulates adipokinetic hormone (Akh) levels in the Akh producing cells
764 (APCs) located at the corpora cardiaca adjacent to the anterior esophagus. HFD also
765 increases APC activity, this results in increased Akh section into the circulation. Akh acts on
766 the Akh receptors (AkhR) expressed by the AkhR cardiac neurons (ACN). The ACN are a pair
767 of neurons located at the posterior end of the adult fly heart, that regulate the heartbeat.
768 Through this signaling pathways, increased Akh under HFD conditions leads to increased
769 arrhythmia.

770

771

772 **FIGURE SUPPLEMENT**

773

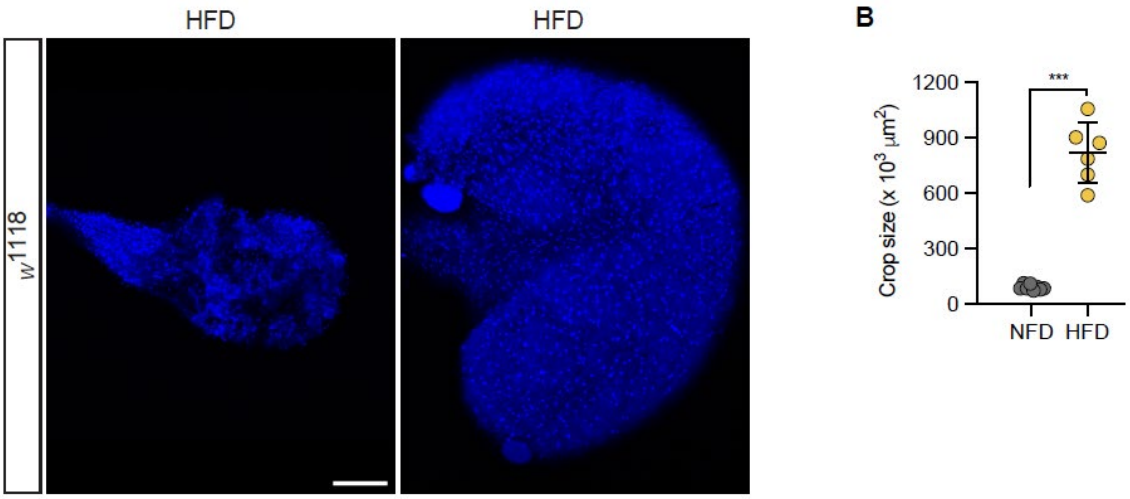

774

775 **Figure 2—figure supplement 1. HFD increases crop size**

776 **(A)** Representative confocal images of crops from female adults (w^{1118}) fed a normal fat diet

777 (NFD) or a high-fat diet (HFD) for 7 days following eclosion from pupa. DAPI stains DNA in

778 blue. Scale bar: 100 μm. **(B)** Quantitation of crop area. n=8 NFD and n=6 HFD. Statistical

779 analysis was performed using *t*-test corrected with Welch; ***, P<0.001.

780